INSTITUTE OF PHYSICS PUBLISHING CLASSICAL AND QUANTUM GRAVITY

Class. Quantum Grav. **20** (2003) 5025–5037 PII: S0264-9381(03)65068-9

# The intrinsic mechanical loss factor of hydroxy-catalysis bonds for use in the mirror suspensions of gravitational wave detectors

**P H Sneddon[1], S Bull[2], G Cagnoli[1], D R M Crooks[1], E J Elliffe[1], J E Faller[3], M M Fejer[4], J Hough[1] and S Rowan[1,4]**

[1] Institute for Gravitational Research, Department of Physics and Astronomy, University of Glasgow, Glasgow G12 8QQ, UK
[2] School of Chemical Engineering and Advanced Materials, University of Newcastle, Newcastle, NE1 7RU, UK
[3] JILA, NIST and University of Colorado, Boulder, CO 80309, USA
[4] Edward L Ginzton Laboratory, Stanford University, Stanford, CA 94305-4088, USA

Received 23 June 2003
Published 17 October 2003
Online at stacks.iop.org/CQG/20/5025

**Abstract**

This paper describes investigations into the mechanical losses of bonds created by hydroxy-catalysis bonding. Evaluation of the magnitude of such losses is important for determining thermal noise levels in bonded suspensions for gravitational wave detectors. Three samples were investigated with bonds of varying geometries and surface areas. In two cases, the bonds were between two pieces of fused silica, whilst in the third a fused silica piece was attached to a sapphire substrate. In each case sodium silicate solution was used as the bonding agent. The thickness and Young's modulus of the bond material were evaluated enabling values for the intrinsic mechanical loss factor of the bonding material to be obtained.

PACS number: 04.80.Nn

## 1. Introduction

Interferometric gravitational wave detectors operate by sensing very small relative displacements of suspended mirrors. Thermal noise from the mirror test masses and their suspensions forms one limit to detector displacement sensitivity in the frequency range from a few tens to hundreds of hertz. Quasi-monolithic test mass suspensions using fused silica fibres jointed to fused silica or sapphire test masses have been adopted [1], or are planned [2] for use in interferometric detectors. These types of suspensions are designed to have very low mechanical loss factors [2], and accordingly very low levels of thermal noise at frequencies of interest. To preserve the low intrinsic loss factors of the suspension requires that the suspension fibres be jointed to the test masses in a way that does not dissipate significant mechanical

  

energy, and is compatible with use in vacuum. The technique of hydroxy-catalysis bonding (or 'silicate' bonding) using potassium hydroxide solution has been used to construct fused silica pendulums of extremely low mechanical loss factors [3]. A variant of this technique which uses sodium silicate solution containing $SiO_2$—which allows successful bonding of surfaces with a greater figure mismatch—has been used to construct the quasi-monolithic fused silica suspensions currently in use in the GEO600 interferometer and is intended for use in the planned upgrade to the LIGO detectors in the US [2, 4].

In previous experiments we have measured the effect of using the hydroxy-catalysis bonding technique on the loss factor of test samples. We then estimated the excess loss associated with the potassium hydroxide bonding and scaled the effect to that expected in full scale suspensions [5]. Here we present experimental results together with associated analysis that allow the intrinsic loss factor of sodium silicate bond material to be determined. These measurements were made at frequencies above 20 kHz. Results on samples made by us and measured by colleagues at Syracuse University over a frequency range lower by a factor of 10 are presented in a separate paper [6].

This is of particular interest, since recent work by Levin [7], amplified by Nakagawa [8] and Yamamoto [9], has shown that spatially inhomogeneous mechanical loss such as that introduced by adding optical mirror coatings, or by bonding ears to the test masses of gravitational wave detectors may introduce levels of thermal noise that are significantly different from those predicted using the modal summation methods that have been commonly used; see for example [10].

## 2. Experimental method

### *2.1. Measurements*

Several experiments were carried out in which the mechanical loss factors for the fundamental longitudinal modes of samples of fused silica and sapphire were measured both before and after the jointing of two such samples or the addition of attachments to the samples by silicate bonding. The fundamental modes were chosen to aid the analysis of the energy distributions in the systems. These energy distributions are required in order to obtain a value of the loss of the bond material.

Assuming all other losses in the system to be negligible, and letting the measured loss factors of the samples before and after the addition of bonded attachments be written as $\phi_{\text{substrate}}$ and $\phi_{\text{bonded}}$, respectively, we may write, for each mode of the sample

$$\begin{aligned}\phi_{\text{bonded}} &= \left(\frac{E_{\text{substrate}}}{E_{\text{total}}}\right)\phi_{\text{substrate}} + \left(\frac{E_{\text{bond}}}{E_{\text{total}}}\right)\phi_{\text{bond}} \\ &\simeq \phi_{\text{substrate}} + \left(\frac{E_{\text{bond}}}{E_{\text{substrate}}}\right)\phi_{\text{bond}}. \end{aligned} \tag{1}$$

By calculating the ratio of the energy stored in the actual bond material, $E_{\text{bond}}$, to the energy stored in the substrate plus the bond, $E_{\text{total}}$ ($\simeq E_{\text{substrate}}$), it is then possible to obtain a value for the loss of the bond material, $\phi_{\text{bond}}$. Three samples were studied, and a value estimated for the loss of the bond material in each case.

Measurements were made of the loss factors of modes of unbonded test masses suspended in vacuum using suspensions of silk thread or wire. Modes of the samples were excited electrostatically and the resulting displacements of the front face of the sample sensed

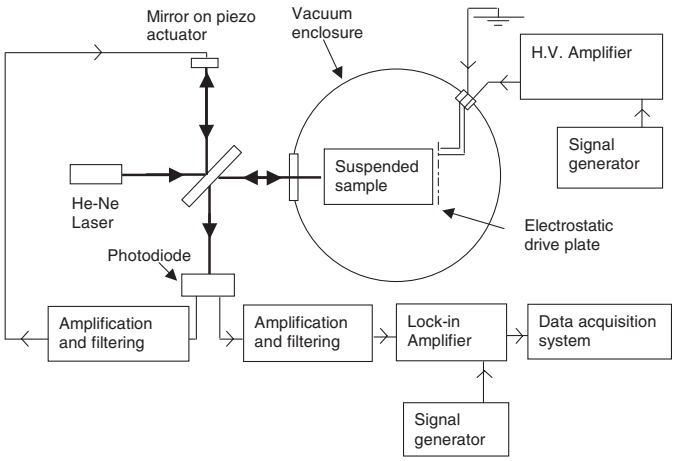


**Figure 1.** Experimental arrangement used to measure the loss factors of suspended test masses.

interferometrically. The arrangement typically used is shown in figure 1 and described in detail by Crooks *et al* [11].

Once a particular mode of a sample was excited to a level significantly above that of its background level, the excitation signal was removed, and the motion of the sample was allowed to decay. The amplitude of the displacement of the front face as a function of time, $A(t)$, was monitored and the loss factor of the mode of the unbonded sample, $\phi(\omega_0)$, was obtained by fitting the envelope of the data to the equation

$$A(t) = A_0 \, \mathrm{e}^{-\frac{\phi(\omega_0)\omega_0 t}{2}}, \tag{2}$$

where $A_0$ is the initial displacement amplitude and $\omega_0$ is the resonant frequency of the mode.

The hydroxy-catalysis bonding technique[5] [5] was then used to, in the first case, bond two identical test masses together to create one larger sample with the same diameter, but twice the length. In the remaining two cases, small fused silica posts or discs were bonded to the sides of the original test masses. A brief description of this technique is given in section 2.2. The specific geometries of the bonded samples studied are shown in figure 2. Each sample was then re-suspended on silk thread and the loss factors of the appropriate modes measured after the addition of the bonded attachments. The measured loss factors for the sample before and after bonding, and the frequencies at which they were measured, are shown in table 1. For each case, several decays were measured and the results averaged. The errors quoted arise from this statistical mean. For case (a), where two pieces of fused silica of equal size were bonded together, the loss of each piece was measured separately before bonding. The best value obtained for the pair was then used as a measure for the 'before' loss.

In each case the addition of a bonded attachment resulted in an increase of the measured loss factors of the modes of the mass studied. This is a result of some of the energy associated with the resonant mode being dissipated by the thin lossy layers of silicate bonding material. In the case of the fused silica samples the additional loss associated with the attached piece itself is negligible as the piece is of essentially the same material as the substrate. In the

[5] Stanford University has a patent for the process of hydroxide-catalysis bonding [12]. Further information on its commercial application can be obtained from Mr Jon Sandelin, Office of Technology Licensing, Stanford University, 900 Welch Road, Suite 350, Palo Alto, CA 94304-1850, USA. E-mail: sandelin@leland.stanford.edu.

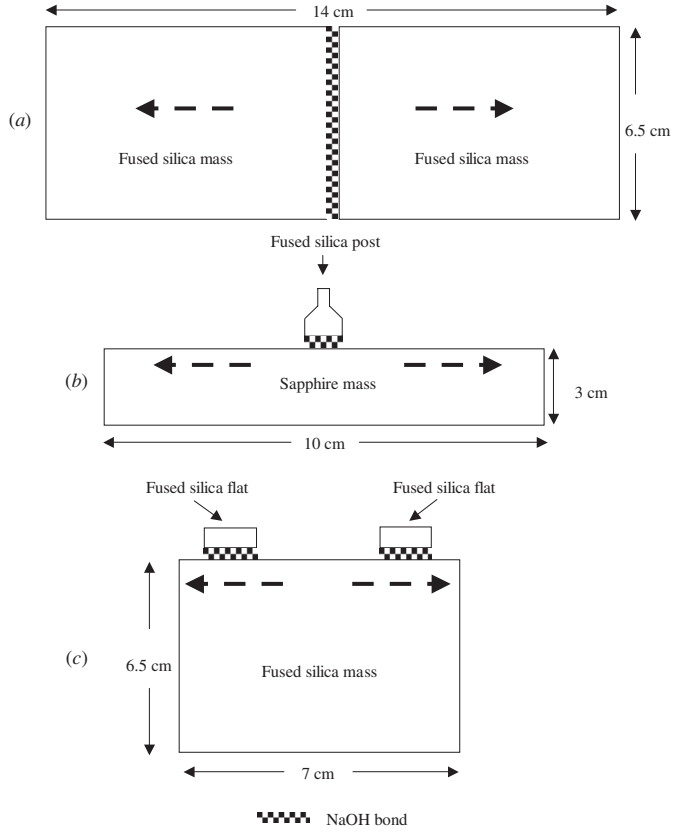


**Figure 2.** Geometries for the three bonded samples investigated. The bond thickness has been exaggerated for clarity.

**Table 1.** Measured loss factors for the fundamental longitudinal modes of samples of fused silica and sapphire taken before and after the addition of silicate bonded attachments.

| Sample | Frequency before bonding (Hz) | Frequency after bonding (Hz) | $\phi_{\text{substrate}}$ | $\phi_{\text{bonded}}$ |
|---|---|---|---|---|
| (a) Silica/silica | 40 050 | 20 411[a] | $(7.1 \pm 0.1) \times 10^{-7}$ | $(3.7 \pm 0.1) \times 10^{-6}$ |
| (b) Silica/sapphire | 53 591 | 53 597 | $(3.9 \pm 0.1) \times 10^{-9}$ | $(3.6 \pm 0.1) \times 10^{-8}$ |
| (c) Silica/silica | 39 730 | 39 639 | $(5.5 \pm 0.2) \times 10^{-7}$ | $(5.9 \pm 0.2) \times 10^{-6}$ |

[a] The change in the frequency shown for the fundamental longitudinal mode is a result of the length of the bonded mass being the sum of the lengths of two individual unbonded masses.

sapphire case, calculations similar to those in section 3.2.2 show that less than 0.1% of the total energy of the resonant mode is stored in the attached piece. Thus the additional loss associated with the presence of this piece is small since the piece itself is made of material with an intrinsic loss of around $10^{-6}$.

**Table 2.** The bonded area, amount and concentration of solution used for each of the bonds studied.

| Case | Bond area ($m^2$) | Amount of bonding solution ($\mu$l) | Proportion of sodium silicate solution to water |
|---|---|---|---|
| (a) Silica/silica | $3.12 \times 10^{-3}$ | 12.50 | 1:4 |
| (b) Silica/sapphire | $5.94 \times 10^{-5}$ | 0.27 | 1:4 |
| (c) Silica/silica | $5.50 \times 10^{-4}$ | 1.50 | 1:6 |

### *2.2. Hydroxy-catalysis bonding*

Hydroxy-catalysis bonding takes place between two surfaces of suitable oxide materials such as silica or alumina or indeed the oxide of any element which forms a salt with the alkali metals.

In general the surfaces to be bonded should be polished to an optical flatness of approximately $\lambda/10$ and be thoroughly cleaned. A sodium silicate solution is then introduced between the two pieces to be bonded and the surfaces then brought together. The sodium silicate solution was produced from a commercial stock solution diluted with water in the ratios as detailed in table 2. The stock solution consists of, in terms of mass, 14% NaOH, 27% $SiO_2$ and 59% $H_2O$. The chemical bonding process is initiated through hydroxide-catalysed surface hydration and dehydration at room temperature. For the case of silica surfaces, bonding with an alkali metal hydroxide, such as potassium or sodium hydroxide, depends on the fact that a number of siloxane bridges (Si–O–Si) are exposed on the polished surfaces of the fused silica. Hydration with the OH ions then activates the bonding surfaces by generating two surface silanol groups (Si–OH) per exposed siloxane bridge (Si–O–Si). Simplistically, the dehydration then strips a water molecule from a pair of surface silanol groups, one on each surface, and forms a siloxane bridge between them and thus a potential bond between the two surfaces. In fact the hydroxide solution also etches the silica and forms silicate ions in the gap between the surfaces. These link together and to the dehydrated silanol groups to form the actual bond between the surfaces. The silicate ions produced act as a filler and allow small mismatches in the surface flatnesses to be accommodated. It is often desirable to supply extra silicate ions to enhance this filling process. This is why a solution of silica in sodium hydroxide, available as sodium silicate solution and used in the bonds described in this paper, makes an excellent bonding agent. It should be noted that repositioning of the pieces being jointed is possible within roughly 30 to 40 s of the start of the jointing process. The maximum bond strength is achieved after several weeks, with the exact time depending on temperature, the concentration of the aqueous solution used and the degree of mismatch of the surface figures of the bonded pieces; however, after only a few hours the bond has sufficient strength to allow the fused silica pieces to be handled for normal purposes.

Table 2 gives details of the area of the bonds created in each of the three cases studied, as well as the amount and concentration of bonding solution used.

## 3. Analytical techniques

To obtain an estimate of the mechanical loss factor of the bonding material, it is necessary to analyse in more detail the distribution of energy stored in the resonating sample. In particular we wish to calculate the fraction of energy stored in the bond layer compared to that stored in the test mass, for the particular geometry studied in each case. All three samples studied were right circular cylinders. Two of these were fused silica and the third sapphire. The specific

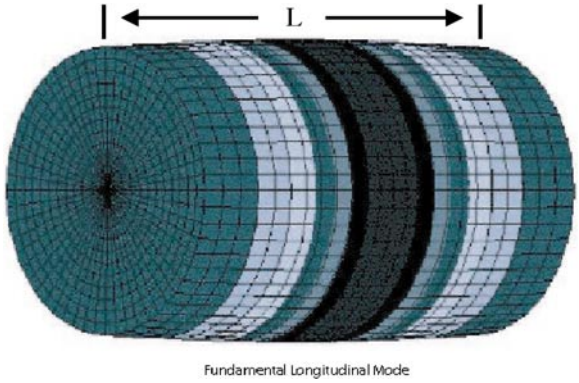


**Figure 3.** Illustration of the shape of the fundamental longitudinal mode of the sample shown in figure 2(*a*). This was obtained using a finite element analysis package (2, $n = 0$ from McMahon [13] symmetry classifications).

sample geometries are shown schematically in figure 2. In each case the mechanical losses measured were for samples resonating in their fundamental longitudinal modes.

As the samples resonate there are essentially forces applied to the bonds by the substrates. These forces are indicated by the dashed arrows in figure 2, and will tend to distort the bonds in tension/compression and/or shear. Here we will assume that the mechanical loss factor associated with different deformations of the bond material is the same. First consider the case in figure 2(*a*).

### *3.1. Bond losses—sample (a)*

In the case shown in figure 2(*a*) the ratio of the energy stored in the bond to that stored in the mass resonating in its fundamental longitudinal mode can be found using simple analytical techniques.

*3.1.1. Energy stored in substrate.* First consider a mass of length $L$ and cross-sectional area $S$ with bond thickness $b \ll L$, with the material properties of the bond being the same as those of the mass. As the mass resonates in its fundamental longitudinal mode, as shown in figure 3, it can be considered to be undergoing simple harmonic motion such that a point at position $x$ anywhere in the $y - z$ plane on the mass, undergoes a displacement $\psi(x) = A\sin(kx)$, where $k = \pi/L$. $x = 0$ is the centre of the bond. If the mass has Young's modulus $Y$, then the energy of a volume element of the same cross-sectional area of the mass and of length d$x$ can be expressed as

$$\Delta E = \tfrac{1}{2} Y S A^2 k^2 \cos^2(kx)\,\mathrm{d}x. \tag{3}$$

Thus the total energy stored in the substrate, $E_{\text{substrate}}$, can be obtained by integration over the length of the bar to give

$$E_{\text{substrate}} = \tfrac{1}{4} Y S A^2 k^2 L. \tag{4}$$

*3.1.2. Energy stored in the silicate bond—sample (a).* Using a similar analysis as for the energy stored in the substrate, the energy stored in the volume of the bond can easily be shown to be

$$E_{\text{bond}} = \tfrac{1}{2} Y S A^2 k^2 b. \tag{5}$$

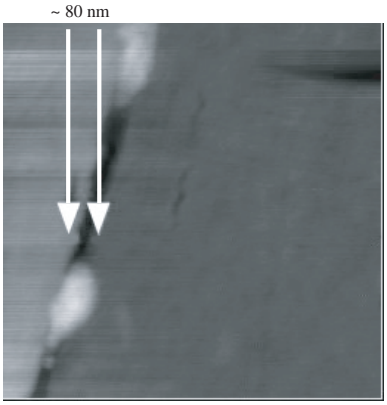


**Figure 4.** Cross-sectional image of a sodium silicate bond obtained using an atomic force microscope. The white areas in the bond are residual polishing compound.

Then allowing for the different Young's modulus for the bond material, as measured in section 3.1.3, the ratio of energy in the bond to energy in the mass becomes (under the assumption that the density of the silicate bond material and the density of the silica mass are equal)

$$\frac{E_{\text{bond}}}{E_{\text{substrate}}} = \frac{2b}{L}\frac{Y_{\text{substrate}}}{Y_{\text{bond}}}. \tag{6}$$

This result is obtained by solving the compressional wave equation for the mass taking into account the different acoustic impedance of the bond region.

*3.1.3. Thickness and Young's modulus of sodium silicate bonds.* To determine appropriate values for bond thickness, $b$, and Young's modulus, $Y$, several bonds were made between pieces of fused silica using sodium silicate solution. The bonds were then cleaved and polished, and studied using an atomic force microscope (AFM). Figure 4 shows a cross section of one of the sodium silicate bonds. Using the AFM, the thickness of the bonds was measured, and the average bond thickness found to be $(81 \pm 4)$ nm. This does not appear to be inconsistent with the surface flatness specification of $\lambda/10$ of the components.

Assessment of the elastic properties of the bond layer was undertaken using the technique of nanoindentation. Using this technique mechanical properties can be measured with high spatial resolution [14]. Load-displacement measurements were made with a Hysitron Triboindenter fitted with a sharp Berkovich diamond indenter (50 nm tip end radius) on the cross section of a sodium silicate bonded assembly with different bond thicknesses at peak loads up to 1 mN. A value for the Young's modulus was obtained for the bond material from the slope of the unloading curve using the method of Oliver and Pharr [14]. Initial results from measurements on thin surface films of the silicate bond material indicated that the elastic modulus of the bond was much less than that of fused silica. In such circumstances the bond region will deflect elastically more than the surrounding silica and care must be taken in the design of the indentation experiment to ensure that the deformation of the bond region is not affected by load support from the surrounding material. Finite element (FE) modelling was undertaken of the nanoindentation testing of an edge-loaded bond to assess the test conditions where reliable data from the bond material could be obtained. This model assumed a Young's modulus of 10 GPa for the bond material (determined from the surface layers). The results

**Table 3.** Parameters needed in the calculation of the bond loss for sample (a).

| Parameters | Sample (a) |
|---|---|
| $Y_{\text{bond}}$ (GPa) | 7.9 |
| $Y_{\text{substrate}}$ (GPa) | $7.2 \times 10^{1}$ |
| $b$ (m) | $8.1 \times 10^{-8}$ |
| $L$ (m) | $1.4 \times 10^{-1}$ |

of the model suggested that a bond thickness of at least 250 nm must be used to ensure that the measurements are not affected in this way. For this reason a 1 $\mu$m thick bond was assessed to avoid the influence of the surrounding fused silica substrate. A Young's modulus of 7.9 GPa, approximately 11% of the value used for bulk fused silica (72 GPa) was obtained. The assumption used here that the properties of the bond layer are constant with thickness is the subject of ongoing research.

*3.1.4. Evaluating the bond loss.* We may rewrite equation (1) as

$$\phi_{\text{bonded}} - \phi_{\text{substrate}} = \frac{E_{\text{bond}}}{E_{\text{substrate}}}\phi_{\text{bond}}. \tag{7}$$

Using the data from tables 1 and 3 in equations (6) and (7), the loss factor of the bond material in this case is found to be $(2.8 \pm 0.4) \times 10^{-1}$. The error on this result is derived from the error on the mean bond thickness and that of the measured mechanical losses.

### *3.2. Studies of bond losses—samples (b) and (c)*

For the fundamental longitudinal modes of samples (b) and (c) of figure 2, the energy stored in each bond is principally shared between that in tension/compression parallel to the plane of the bond, $E_{\text{tension}}$, and that in shear of the bond, $E_{\text{shear}}$. The total energy stored in the bond, therefore, can be expressed as

$$E_{\text{bond}} = E_{\text{tension}} + E_{\text{shear}}. \tag{8}$$

It is therefore possible to revise equation (1) in the following way:

$$\phi_{\text{bonded}} \simeq \phi_{\text{substrate}} + \phi_{\text{bond}} \left( \frac{E_{\text{tension}} + E_{\text{shear}}}{E_{\text{substrate}}} \right). \tag{9}$$

Using appropriate values for $E_{\text{tension}}$, $E_{\text{shear}}$ and $E_{\text{substrate}}$, along with measured values for $\phi_{\text{bonded}}$ and $\phi_{\text{substrate}}$ we may obtain values for $\phi_{\text{bond}}$ for samples (b) and (c). The simple symmetry of the bond in sample (a) made evaluation of the ratio of energy stored in the bond to the mass using analytical techniques straightforward. For the geometries of bonds in samples (b) and (c) the situation is more complicated and so here a combination of FE and analytic treatments are used to evaluate $E_{\text{tension}}$ and $E_{\text{shear}}$.

*3.2.1. $E_{\text{tension}}$ in a circular bond—sample (b).* Consider the sample in figure 2(*b*) oscillating in its fundamental longitudinal mode. Again let the top surface of the mass to which the bond is attached be considered as undergoing simple harmonic motion such that a point at position $x$ on the mass, where $x = 0$ is the centre of the bond, as detailed in figure 5, undergoes a displacement $\psi(x) = A\sin(kx)$, where $k = \pi/L$.

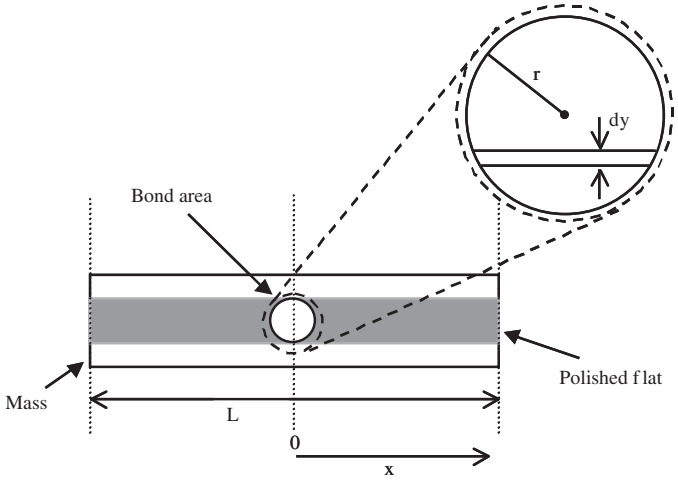


**Figure 5.** Schematic diagram showing bonded area on sample (b).

Let the bond be of radius $r$ and thickness $b$, and composed of elements of width $\mathrm{d}y$. Energy density can be expressed as $\frac{1}{2} \times$ stress $\times$ strain. Then the energy in a strip of length $2x$, thickness $b$ and width $\mathrm{d}y$, can be expressed as

$$\Delta E = Y_{\mathrm{bond}}\, \mathrm{d}y\, x b A^2 k^2, \tag{10}$$

assuming that $x \ll L$, the length of the mass. Changing to circular coordinates, such that $x^2 + y^2 = r^2$, and integrating over the area of the bond gives

$$E_{\mathrm{tension}} = Y_{\mathrm{bond}}\, b A^2 k^2 \frac{\pi r^2}{2}. \tag{11}$$

*3.2.2. $E_{\mathrm{shear}}$ in a circular bond.* The shear strain, $\theta$, at any point in the bond is related to the parallel tensile/compressional displacement of the bond and can be expressed as

$$\theta = \alpha \psi(x), \tag{12}$$

where $\alpha$ is a constant whose magnitude is a function of the properties of the bond and the attachment. The FE program Ansys[6], was used to evaluate $\alpha$ for the geometry studied here. However because of the very thin nature of the bond it was not possible to do this directly. Instead a tangential force was applied along the bonded face of the attachment symmetric about the middle of the bond such that the attachment was effectively stressed in the same way as when the mass oscillates in its fundamental longitudinal mode. Figure 6 shows a profile view of the fused silica post from sample (b) with such a force applied.

The image shows only the right-hand half of the cylinder, whose base is simulated to be in contact with the resonating mass. The distortion of the lower region of the bonded attachment is clear. The average displacement at the end of the bond was then measured as a function of depth into the attachment. From a graphical analysis of this, the shear strain at the surface can be found. The ratio of this shear strain to the surface displacement is a measure of $\alpha$ for the case where the bond is made of the same material as the attachment. The value of $\alpha$

[6] Ansys is available from Wilde and Partners Ltd, Brindley Lodge, Adcroft Street, Stockport SK1 3HS, UK or via http://www.WildeAndPartners.co.uk.

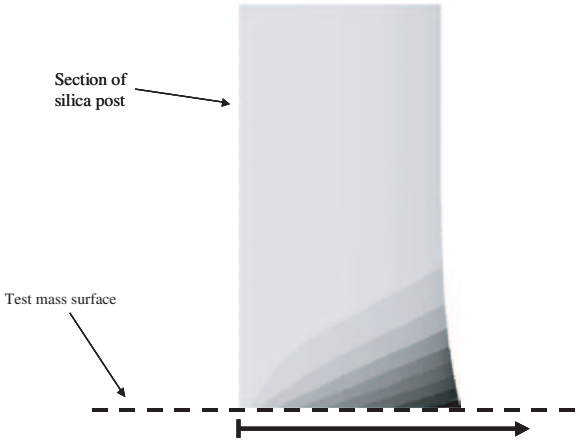


**Figure 6.** FE model of one half of a fused silica post distorted by the motion of a resonating mass. Regions of increasing stress are indicated by darker shading.

**Table 4.** Parameters needed in the calculation of the bond loss for sample (b).

| Parameters | Sample (b) |
|---|---|
| $Y_{\text{bond}}$ (GPa) | 7.9 |
| $G_{\text{bond}}$ (GPa) | 3.95 |
| $Y_{\text{substrate}}$ (GPa) | $3.98 \times 10^{2}$ |
| $b$ (m) | $8.1 \times 10^{-8}$ |
| $S(\text{m}^2)$ | $7.07 \times 10^{-4}$ |
| $L$ (m) | $1 \times 10^{-1}$ |
| $r$ (m) | $4.5 \times 10^{-3}$ |
| $\alpha$ | $4.48 \times 10^{3}$ |

for the actual bond material was obtained by scaling using the relevant mechanical properties of the bond material and the material of the attachment.

Using standard finite element techniques the mesh size of the finite element model was varied until the value for $\alpha$ converged to a value of $4478 \pm 88$ for case (b). (Here the error arises from the extrapolation involved in the model convergence.) Now, since $\theta = \alpha\psi(x) = \alpha A \sin(kx)$, the expression derived for $E_{\text{shear}}$, using methods similar to those previously used, is

$$E_{\text{shear}} = \frac{1}{3} G_{\text{bond}} b \alpha^2 A^2 k^2 \frac{3\pi}{8} r^4, \tag{13}$$

where $G_{\text{bond}}$ is the shear modulus of the bond material. Then combining equations (4), (11), and (13) gives

$$\frac{E_{\text{bond}}}{E_{\text{substrate}}} \simeq \frac{2\pi r^2 b}{Y_{\text{substrate}} SL} \left[ Y_{\text{bond}} + \frac{G_{\text{bond}} \alpha^2 r^2}{4} \right]. \tag{14}$$

The parameters used to evaluate $\phi_{\text{bond}}$ using equations (1) and (14) are summarized in tables 1 and 4. Note, the shear modulus of the bond material, $G_{\text{bond}}$, was approximated as $Y_{\text{bond}}/2$, thus ignoring any effect of Poisson's ratio which we expect to be small. Then $E_{\text{bond}}/E_{\text{substrate}} = (1.5 \pm 0.2) \times 10^{-7}$, giving a bond loss of $(2.1 \pm 0.3) \times 10^{-1}$. For this case,

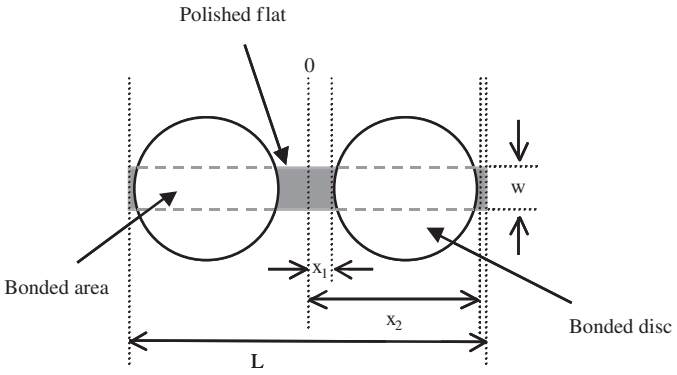


**Figure 7.** Schematic diagram of sample (c). The diameters of the bonded pieces were greater than the width of the flat on the fused silica mass, producing roughly rectangular bonds.

the errors are derived from the error on the mean bond thickness, the uncertainty in the $\alpha$ factor and the statistical mean of the measured losses.

*3.2.3. Energy stored in two rectangular bonds—sample (c).* Here we deal with the case where each bond is approximately rectangular in shape, of width $w$, thickness $b$ and positioned between $x_1$ and $x_2$ and $-x_1$ and $-x_2$ as detailed in figure 7. Following the same procedure as above the following expressions can be derived:

$$E_{\text{tension}} = \frac{1}{2} Y_{\text{bond}} bw A^2 k^2 \left[ (x_2 - x_1) + \frac{\sin(2kx_2) - \sin(2kx_1)}{2k} \right], \tag{15}$$

and

$$E_{\text{shear}} = \frac{1}{2} G_{\text{bond}}\, bw\alpha^2 A^2 \left[ (x_2 - x_1) - \frac{\sin(2kx_2) - \sin(2kx_1)}{2k} \right]. \tag{16}$$

*3.2.4. Energy ratio for the rectangular case.* Recalling equation (4), the ratio is

$$\frac{E_{\text{bond}}}{E_{\text{substrate}}} = \frac{2bw}{YSk^2L} \Upsilon, \tag{17}$$

where,

$$\Upsilon = k^2 Y_{\text{bond}} \left[ (x_2 - x_1) + \frac{\sin(2kx_2) - \sin(2kx_1)}{2k} \right] + \alpha^2 G_{\text{bond}} \left[ (x_2 - x_1) - \frac{\sin(2kx_2) - \sin(2kx_1)}{2k} \right]. \tag{18}$$

The relevant parameters needed to evaluate $\phi_{\text{bond}}$ using equations (1) and (17) are summarized in tables 1 and 5. Note that $\alpha$ for this geometry was evaluated using FE techniques as described previously and in this case found to be $1405 \pm 71$.

The ratio of energy stored in the bond to energy stored in the mass, $E_{\text{bond}}/E_{\text{substrate}}$, is thus $(1.1 \pm 0.1) \times 10^{-5}$ and the mechanical loss of the bond material, $\phi_{\text{bond}}$, found to be $(4.9 \pm 0.5) \times 10^{-1}$. These errors arise from the same sources as in case (b).

**Table 5.** Parameters needed in the calculation of bond loss for sample (c).

| Parameters | Sample (c) |
|---|---|
| $Y_{\text{bond}}$ (GPa) | 7.9 |
| $G_{\text{bond}}$ (GPa) | 3.95 |
| $Y_{\text{substrate}}$ (GPa) | $7.2 \times 10^{1}$ |
| $b$ (m) | $8.1 \times 10^{-8}$ |
| $L$ (m) | $7 \times 10^{-2}$ |
| $w$ (m) | $1.1 \times 10^{-2}$ |
| $S(\text{m}^2)$ | $3.32 \times 10^{-3}$ |
| $x_1$ (m) | $5 \times 10^{-3}$ |
| $x_2$ (m) | $3.1 \times 10^{-2}$ |
| $\alpha$ | $1.41 \times 10^{3}$ |

**Table 6.** Summary of results for the three bonded samples.

| Sample | $\phi_{\text{bond}}$ |
|---|---|
| (a) | $(2.8 \pm 0.4) \times 10^{-1}$ |
| (b) | $(2.1 \pm 0.3) \times 10^{-1}$ |
| (c) | $(4.9 \pm 0.5) \times 10^{-1}$ |

## 4. Summary and conclusions

Table 6 summarizes the bond losses calculated above.

From the experiments and analysis described above it can be seen that the loss factor for silicate bonding material falls in the range of $1.8 \times 10^{-1}$ to $5.4 \times 10^{-1}$. It is interesting to note that there appears to be a higher loss for the case where the bonding solution ratio was 1:6 (case (c)), as opposed to 1:4 (cases (a) and (b)). This variation in loss will be investigated in future experiments.

The direct sources of errors in the results for mechanical loss have been discussed where appropriate at various points in the text. However, there remains the possibility of systematic errors associated with using simple analytical models for the mechanical systems. To make a simple check for this, the energy ratio for case (a) was also evaluated using finite element analysis and then compared with that obtained from the analytical model. The energy ratios were found to be within 10% of each other and thus the systematic error is smaller than the quoted experimental error. A similar level of systematic error is expected for the other cases and will not be discussed further.

The bond losses are quite high compared with typical values for the intrinsic loss of fused silica. However, the silicate bond material can be thought of as forming a very imperfect glass with many vacancies, dislocations and incomplete bond and it should be noted that some well-formed glasses have loss factors that are only 50 times better [15] than this bond material. Further only a very small quantity of material is required to fabricate the mirror suspensions and this material is located at some distance from the reflecting surface of the mirror. Modern methods of evaluation of thermal noise [7–9] require knowledge of the spatial distribution and level of the mechanical losses in the suspension system. The results here are significant as they will contribute to the evaluation of the thermal noise in the mirror suspension systems being designed for gravitational wave detectors.

## Acknowledgments

The authors are very grateful to Dr Jamie Scott of the Solid State Physics Group in Glasgow University for help with using the atomic force microscope. We would like to thank PPARC in the UK and the NSF in the US (award NSF-PHY-0140297) for financial support along with the Universities of Stanford, Glasgow and Newcastle. We also wish to acknowledge our colleagues in the GEO 600 Project and at Stanford University for their interest in this work.

## References

[1] Willke B *et al* 2002 *Class. Quantum Grav.* **19** 1377–87
[2] Robertson N A *et al* 2002 *Class. Quantum Grav.* **19** 4043–58
[3] Tokmakov K, Mitrofanov V, Braginsky V, Rowan S and Hough J 1999 *Proc. 3rd E. Amaldi Conf. on Gravitational Waves* (Pasadena, CA: AIP) pp 445–56
[4] Gustafson E, Shoemaker D, Strain K and Weiss R 1999 *LIGO* T990080-00-D (LSC White Paper on Detector Research and Development)
[5] Rowan S, Twyford S M, Hough J, Gwo D-H and Route R 1998 *Phys. Lett.* A **246** 471–8
[6] Smith J R, Harry G M, Betzwieser J C, Gretarsson A M, Guild D A, Kittelberger S E, Mortonson M J, Penn S D and Saulson P R 2003 *Class. Quantum Grav.* **20** 5039–47
[7] Levin Y 1998 *Phys. Rev.* D **57** 659
[8] Nakagawa N, Gretarsson A M, Gustafson E K and Fejer M M 2002 *Phys. Rev.* D **65** 102001
[9] Yamamoto K 2000 Study of the thermal noise caused by inhomogeneously distributed loss *PhD Thesis* University of Tokyo
[10] Gillespie A and Raab F 1995 *Phys. Rev.* D **52** 577–85
[11] Crooks D R M *et al* 2002 *Class. Quantum Grav.* **19** 883–96
[12] Gwo D-H 2001 Ultra precision and reliable bonding method *United States Patent* no US 6284085 B1
[13] McMahon G W 1964 *J. Acous. Soc. Am.* **36** 85
[14] Oliver W C and Pharr G M 1992 *J. Mater. Res.* **7** 6
[15] Kimball A L and Lovell D E 1927 *Phys. Rev.* **30** 955